Optics & Laser Technology

Volume 22 Number 1 February 1990

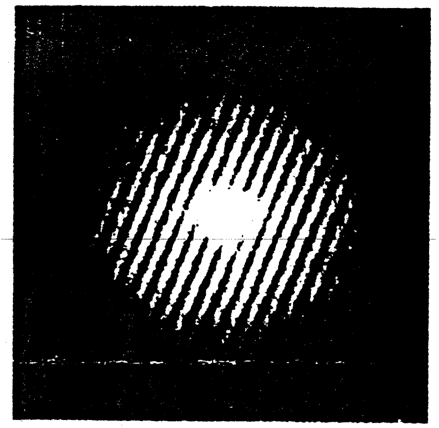

Cover Picture

A typical fringe pattern generated by a specklegram using the point-wise technique. The diffracted light projected on to the screen takes the form of a circular halo modulated by a pattern of equally spaced fringes normal to the local displacement vector. **See the article by Barbero et al on page 17.**

It should be noted that all articles submitted to *Optics and Laser Technology* will be refereed by at least one international independent expert, and that no page charges are levied

Fracture analysis of a surface-coated ceramic by speckle photography and finite elements

E.J. BARBERO, G.H. KAUFMANN, S.R. IDELSOHN

The fracture behaviour of a four-point bend surface-coated ceramic specimen with a through-the-thickness crack was experimentally investigated. Speckle photography was used to measure opening displacements over the specimen surface and across the crack line. For a glazed and unglazed specimen, stress-intensity factors were experimentally determined by means of a method that uses data not restricted to the singularity-dominated zone. Stress-intensity factors were numerically calculated using a three-dimensional finite element analysis and their variations along the crack front were also evaluated. Experimental results agree reasonably well with the numerical results. Results show the influence of the glaze on the fracture behaviour of the composite material.

KEYWORDS: speckle (photography), fractures, ceramics, stress measurement

Introduction

Linear elastic fracture mechanics has provided powerful methods for evaluating the effect of defects on the fracture properties of brittle materials. The stress-intensity factor is a parameter which provides a characterization of the stress field near a crack tip required to cause failure[1]. This stress field can be related to the applied stress on the structure, the material properties and the defect size. Brittle fracture occurs whenever the stress-intensity factor reaches a critical value due to either an increase in the applied stress or a growth in the crack length or both. This value, representative of the material, is called the fracture toughness. Since the fracture design of brittle components requires the determination of the stress-intensity factor, considerable effort was expended in the development of suitable numerical solutions for realistic geometries[2]. Frequently significant idealizations are required for the numerical analysis, so experimental evaluation of this parameter is of considerable importance. Because of the increasing use of ceramic materials for critical structural applications, extensive work was done in this area in recent years.

EB and SI are in the Instituto de Desarrollo Tecnológico para la Industria Quimica (CONICET-UNL), Guemes 3450, 3000 Santa Fe, Argentina; GHK is in the Instituto de Fisica Rosario (CONICET-UNR), Bv. 27 de Febrero 210 bis, 2000 Rosario, Argentina. Received 13 June 1989. Revised 22 August 1989.

This paper presents an experimental and numerical investigation on the fracture behaviour of a surface-coated ceramic. These two-phase materials, as in the case of high voltage porcelain insulators, are coated with a glaze that is usually weaker than the underlying ceramic. However, higher strengths are found with a glaze that has a lower thermal expansion coefficient than the ceramic[3]. This places the glaze under a compressive stress when the composite specimen is cooled in the manufacturing process. In this way, an increase in strength of about 30% can normally be obtained.

As fracture mechanics is essentially a continuum mechanics concept, one of the motivations of this work is to show that this approach can be applied to study multiphase ceramic materials, such as electrical porcelain. Furthermore, the stress field created by the glaze over the specimen surface induces a variation of the stress-intensity factor along the crack front. So a three-dimensional analysis that accounts for this effect is needed. For this reason, another motivation of this work is to present an experimental evaluation of three-dimensional finite element calculations in a surface-coated ceramic specimen with a through-the-thickness crack.

The experimental evaluation was accomplished by speckle photography[4]. The use of this technique for displacement and strain measurement has developed rapidly in the past decade. Its use in fracture mechanics offers several advantages. As with other coherent optics techniques, it is non-contact. If the speckle pattern is created by a laser, the model surface needs no preparation. It does not require materials with special optical characteristics, so it can be directly applied to prototype materials. The determination of fracture parameters using speckle photography seems to have been introduced by Evans and Luxmoore[5], who measured the displacement field around a crack tip in a single edge notch tension specimen. Several authors used this technique to calculate stress-intensity factors for different types of cracks[6-8]. More recently it was used jointly with holographic interferometry to evaluate three-dimensional finite element calculations in an internally pressurized cylinder with an external part-circular crack[9].

In the next section, we describe the specimen used in the tests and give details of the application of the speckle photography technique. Then, we present the finite element model and the method, used to calculate the stress-intensity factors, which uses data not restricted to the singularity-dominated zone. Experimental and numerical results of opening displacements are compared for both unglazed and glazed specimens. For the unglazed specimen, stress-intensity factors calculated from experimental and numerical results are compared with a well-known analytical solution. The variation of the stress-intensity factor along the crack front is also evaluated.

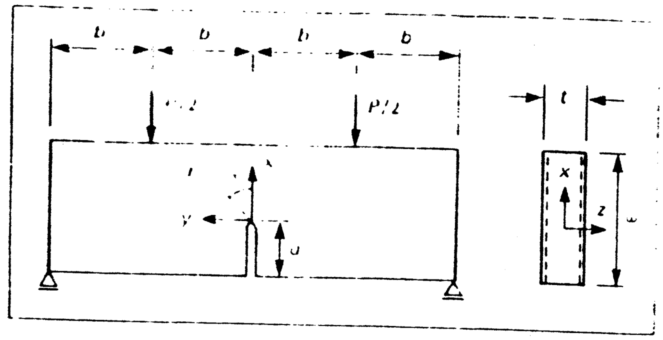

Fig. 1 Specimen geometry

Table 1. Mechanical properties

Material	Young's Modulus E (Pa)	Poisson's Ratio ν	Coefficient of linear thermal expansion α (°C^{-1})
Porcelain	7.28×10^{10}	0.3	5.5×10^{-6}
Glaze	5.6×10^{10}	0.3	4.8×10^{-6}

Experimental details

Specimen

A four-point bend specimen was used for the experiments, so that only the fracture mode I exists. The material was an electrical silico-aluminous porcelain. The test bar was made by wet process, glazed with a standard brown enamel of average thickness 0.096 mm and fired in a tunnel kiln at a temperature of 1300°C. The bar has a length $4b$ of 125 mm, a width w of 40 mm and a thickness t of 12 mm as shown in Fig. 1. To simulate a crack, a through-the-thickness 0.3 mm wide slot terminating in a vee notch with a 30° flank angle was transversely inserted at the specimen half-length with a diamond saw. The crack length a is 17 mm.

The bend test fixture was built to conform with ASTM specifications[10], except that four-point instead of three-point loading was applied. It was designed to minimize errors which can arise from friction between the specimen and the supports. The support rolls are allowed limited motion along plane surfaces, but are initially positioned against stops using rubber bands.

To get a flat surface for assuring a good contact between the bar and the support rolls, the specimen was polished by machining. Prior to the test, the specimen was annealed at 200°C for three hours to remove the residual stress. Then, the area surrounding the crack was sprayed with a thin coat of matt white paint, which acted as a scattering surface for the speckle technique.

Table 1 shows the mechanical properties of both materials, porcelain and glaze.

The specimen was strained in a special loading frame. The load was applied by screw action and was measured by a calibrated load cell.

Speckle photography

A usual optical set-up was used to record the double-exposure specklegrams[4]. The specimen surface was illuminated with a divergent beam of HeNe laser light and was imaged by means of a well-corrected camera lens on to a SO-253 Kodak photographic plate mounted parallel to it. A 210 mm focal length of aperture $F = 2.8$ was used at a magnification $m = 2.5$.

Displacement information was recovered using a pointwise technique by sending a narrow laser beam through the double-exposure specklegram at the point of interest. The diffracted light projected on a screen takes the form of a circular halo modulated by a pattern of equally spaced fringes normal to the local displacement vector (Fig. 2). By measuring the spacing and orientation of the fringe pattern, the in-plane displacement components d_x and d_y can be calculated[4].

The d_x displacements measured along the crack line were very small, about a few micrometres; these were below the basic sensitivity of the technique. It can be shown that the sensitivity is limited by the average speckle size, so that displacements to be measured must be greater than[4]

$$s = 1.22\lambda F(1+m)/m \tag{1}$$

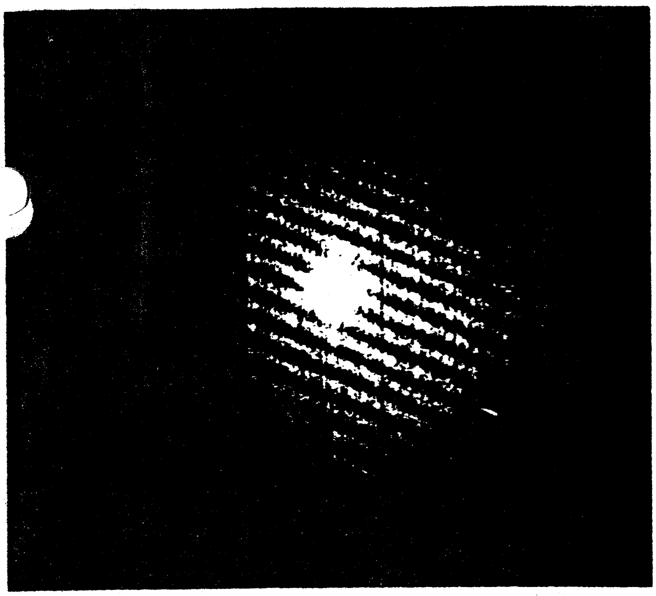

Fig. 2 Typical fringe pattern generated by specklegram using the point-wise technique

where λ is the wavelength of the laser. In our experiments s was about 3 μm. For this reason, the sensitivity was increased by superimposing a small artificial displacement of about three times the speckle size. As in a previous work[7], it was produced by mounting the photographic camera on a precision translation stage.

The speckle photography technique was used to measure the crack opening displacement u_y over the specimen surface along the slot line ($\theta = \pi$). It was determined as follows[7]. First, the spacing and the orientation of the fringes generated when the laser beam scanned the specklegram along two lines parallel to the slot direction were measured. These lines, one at each side of the crack, stood at a distance of 0.5 mm from the slot. Second, d_y displacements perpendicular to the crack line were determined for points along both lines. Finally, the crack opening displacement u_y was calculated as one half of the difference between the d_y displacements corresponding to a pair of opposite points at each side of the slot having the same distance r. In this way, the rigid body displacement used to increase the sensitivity was cancelled when this difference was made.

It is known that speckle decorrelation effects due to out-of-plane displacements can arise, causing a decrease in fringe visibility which can lead to errors[4]. Theory predicts that this movement must be smaller than

$$\Delta z = 4\lambda F^2(1 + m)^2/m^2 \qquad (2)$$

not to obtain appreciable fringe degradation. In this work Δz was about 0.04 mm, so great care was required in keeping the specimen movement to one plane when it was stressed. For this purpose, two guideways were included in the loading frame.

Tests

In a ceramic material, measurements of any physical parameter exhibit a spread of results when a series of tests is conducted in different specimens under nominally similar conditions. Neglecting measurement errors associated with any test method, there is a genuine variation from specimen to specimen in the property being measured. These variations are due to minor differences in raw materials or in the manufacturing process. A factor of major significance includes the temperature of the furnace and the temperature gradients within it. Variations of ±20% from the mean value of a given property are typically recorded on different samples.

For this reason, measurements were done on the same sample. First, crack opening displacements were measured on the glazed specimen for different loads. Then, the glaze was taken out by polishing with a silicon carbide disc rotating at low speed. The specimen was refrigerated with water during the polishing process to prevent the generation of high thermal stresses. Before testing again, the specimen was annealed and sprayed with white paint. Once more, crack opening displacements were measured on the unglazed specimen for different loads. To avoid the variation of mechanical properties from sample to sample, the elastic moduli of the porcelain were measured using a bar which was cut from the unglazed specimen.

Finite element analysis

Three-dimensional finite element calculations were performed to be compared with experimental results. Two types of elements were used to model the finite-thickness specimen. Isoparametric 16-node elements were used everywhere except in the vicinity of the crack front. This element has a quadratic displacement field over the specimen surface and a linear one across the thickness. It was found that the use of a quadratic displacement field across the thickness did not improve results but only increased computing costs. Collapsed quarter-point isoparametric elements were located around the crack front. These singularity elements had square-root terms in their assumed displacement field and therefore produced a singular stress field at the crack front[11]. As shown in Fig. 3, singularity elements size was chosen for including the zone where the stress field singularity was important. In

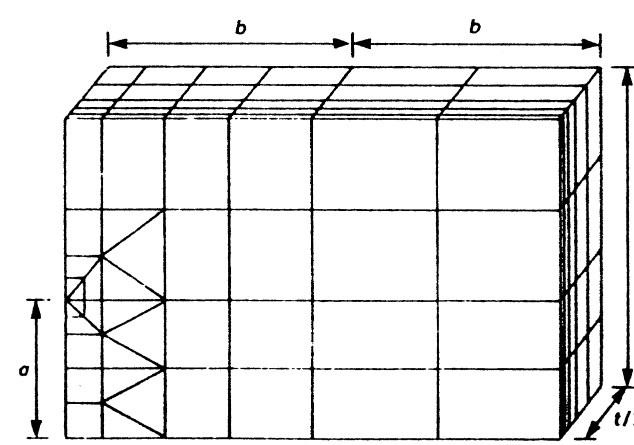

Fig. 3 Finite-element mesh (element size is not to scale in the thickness direction)

this way, it was not necessary to use transition elements between the singularity ones and those which were used to idealize the rest of the specimen.

In order to study the convergence of the solution, several two-dimensional mesh idealizations were analysed. A stress-intensity factor that agrees within 3% of one calculated by Bueckner[12, 13] was obtained for the unglazed specimen. Bueckner's solution is a well-known analytical solution which is obtained using integral equation procedures. It agrees closely with values calculated by other numerical methods such as boundary collocation and those determined from compliance measurements.

The two-dimensional mesh was used to generate a three-dimensional one, modelling the thickness of the specimen with ten non-uniform layers. Because of symmetry, only a quarter of the specimen was idealized, applying symmetry boundary conditions on the $y = 0$ and $z = 0$ planes. The used mesh had 195 elements and 2145 degrees of freedom.

Because of thickness, the glaze was idealized with one layer of elements. Four non-uniform layers were used to idealize the underlying ceramics. In this way the boundary layer effect that is produced by the glaze on the specimen surface can be satisfactorily approximated[14]. The layer thicknesses from the mid-plane to the surface were $0.205t$, $0.205t$, $0.041t$ and $0.08t$.

The thermal stress field on the glaze introduced during the manufacturing process was first calculated by using the linear thermal expansion coefficients of both materials listed in Table 1. This stress field was converted to equivalent nodal forces in order to find a displacement field. Finally, this was superimposed upon the displacement field corresponding to the applied load for obtaining the resultant displacements.

The computer program SAMCEF[15] was used for the numerical analysis.

Stress-intensity factor evaluation

In the case of a plate with a through-the-thickness slot, the state of deformation varies in the thickness direction as well with the distance from the slot front. The use of the plane strain assumption to evaluate the stress-intensity factor is only justified near the middle of the finite-thickness specimen where that condition may exist but not over its free surface. For these reasons, the evaluation of this parameter from the measurement of surface displacement is a controversial issue. As in this work we are mainly interested in a comparative study between the glazed and the unglazed specimens, we assume the presence of an inverse square root singularity in the stresses at the free surface and a plane stress behaviour for displacements near the crack tip.

Plotting crack opening displacements against $r^{1/2}$ for experimental data points that have $r < 0.1\,a$, a straight line can be fitted whose slope yields the mode I stress-intensity factor[16]. However, errors resulting from imperfections in the crack tip geometry and departures from the basic assumptions of linear fracture mechanics can arise for displacement data near the crack tip. Also, important errors can arise if a very low number of data points are available. For these reasons, some methods were recently developed to use data not restricted to the singularity-dominated zone[17, 18].

In this work we used the method introduced by Baker et al[18], which can be briefly described as follows. The stress components are obtained from an Airy stress function that is expressed as a truncated power series. For the case of plane stress, the u_y displacement can be expressed as

$$u_y = \sum_{l=0}^{L} S_l(r, \theta) C_l \tag{3}$$

where L is the number of terms in the stress-function expansion, $S_l(r, \theta)$ are known functions of position and C_l are the unknown coefficients of the stress function. Retention of the first term in (3) leads to the well-known near-field equation and

$$C_0 = K_I / \sqrt{2\pi} \tag{4}$$

In principle, it is possible to select $L + 1$ data points and to directly solve the equations. However, to minimize errors a least squares method was used and Q data points (where $Q > L + 1$) were employed.

Results and discussion

Fig. 4 shows the opening displacement u_y that were measured over the specimen surface and along the crack line. They are plotted against r, where r is the distance to the crack front. These displacements were measured from the same specimen, with and without glaze, and for a load of 382 N. For the unglazed specimen, it is seen that crack opening displacements near the crack front are greater than those measured for the glazed specimen. These results were expected and they are due to the

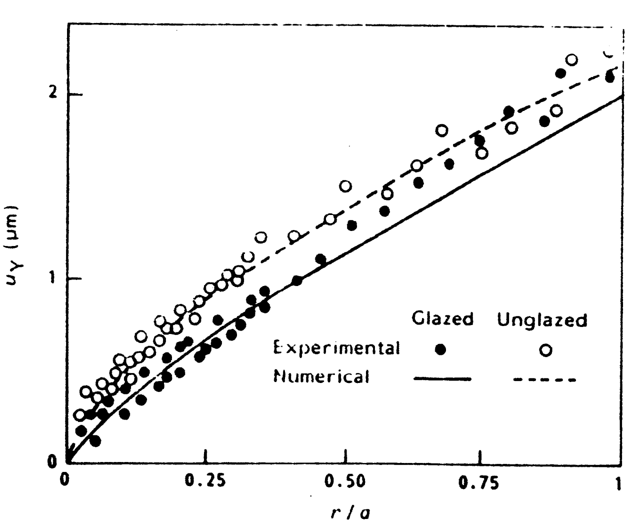

Fig. 4 Opening displacement u_y along the crack line

compressive stress field created by the glaze. Far from the crack front, displacements for both specimens coalesce.

Crack opening displacements that were calculated over the specimen surface and along the crack line from the three-dimensional finite element analysis are also shown in Fig. 4. Considering that the specimen was not perfectly plane and its width had a 5% variation, it is seen that a reasonable agreement between experimental and numerical results was obtained.

To calculate the stress-intensity factor, four terms in the stress-function expansion were used to model the displacement field. Using a series of numerical experiments, Barker et al[18] confirmed that the addition of the next higher order term did not drastically improve the results. Crack opening displacements that were measured along the crack line for $r < 0.3a$ (about 25 data points) were used to calculate K_I. For the unglazed specimen, a value $K_I = 5.49 \times 10^5\ \mathrm{Nm}^{3/2}$ was obtained. This value compares well with that one of $5.66 \times 10^5\ \mathrm{Nm}^{3/2}$ obtained from Bueckner's solution[12].

For the glazed specimen, an effective stress-intensity factor can be defined by using the elastic constants of the underlying ceramic. From experimental data, a value $K_{I\,ef} = 4.64 \times 10^5\ \mathrm{Nm}^{3/2}$ was obtained.

The stress intensity factor variation across the thickness obtained from the three-dimensional finite element model is shown in Fig. 5. For a particular location along the crack front, the stress-intensity factor was computed by means of the same procedure previously used to calculate K_I from experimental data. The stress-intensity factor for the unglazed specimen is found to be nearly uniform across the thickness and only a 1% variation is obtained. A value $K_I = 5.56 \times 10^5\ \mathrm{Nm}^{3/2}$ is calculated at the free surface, which compares well with the experimental one of $5.49 \times 10^5\ \mathrm{Nm}^{3/2}$.

For the glazed specimen, numerical results show

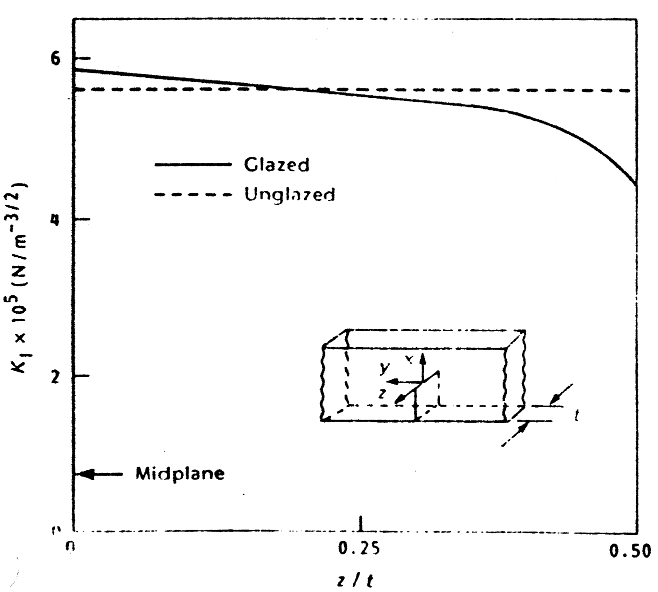

Fig. 5 Distribution of stress-intensity factor across thickness obtained from finite-element results

that the effective stress-intensity factor lightly increases at the mid-plane but drops off rapidly at the free surface. The value $K_{I\,ef} = 4.42 \times 10^5\ \mathrm{Nm}^{3/2}$ calculated at the free surface from the present analysis is in reasonable agreement with that of $4.64 \times 10^5\ \mathrm{Nm}^{3/2}$ experimentally obtained. The difference between numerical and experimental results at the surface of the glazed specimen could be due to variations of the thermal expansion coefficients, which prove to have a significant effect on the results. For any technological application, either a better measurement of these coefficients or a calibration of their value with the techniques here described may be necessary.

To conclude, we will discuss the influence of speckle photography errors on the stress-intensity factor computation, assuming that the specklegram is recorded at a known scale factor and free of any optical distortion. The measurement of the specklegram coordinates associated to the point illuminated by the laser beam introduces errors. Other errors also appear in relation to the measurement of fringe spacing and orientation. These are referred to as random errors because they become smaller if a large number of measurements are taken. A systematic position error is also introduced if the coordinate system origin, which shall coincide with the crack tip, is not located exactly. This last error is present in all the data.

To evaluate the accuracy of the stress-intensity factor determination, the value for the unglazed specimen was recalculated as follows. Each displacement u_y and radial coordinate r used as input for the evaluation of K_I were shifted by a random amount according to the equations

$$u_y = u_y + n_1 \Delta u_y \tag{5}$$

$$u_y = u_y + n_2 \Delta r \tag{6}$$

where n_1 and n_2 are two random number distributions, mutually independent, in the range ± 1. Due to the accuracy of the speckle photography technique, the maximum random error in displacements was taken as $\Delta u_y = 0.2\,\mu\mathrm{m}$. As x and y coordinates of data points can be located over the specklegram with an accuracy of 0.25 mm, the maximum random error in the radial distance from the crack tip was taken as $\Delta r = 0.5$ mm. To take into account the error introduced in locating the crack tip, the coordinate system was shifted in 0.25 mm along both x and y axes about the crack tip used in previous calculations.

As a result of this analysis, a stress-intensity value that differs by 6% from that computed previously was obtained. Thus, we conclude that this value is the average error with which stress-intensity factors were evaluated in this work.

Conclusions

The use of speckle photography to measure surface opening displacements along a through-the-thickness crack in unglazed and glazed porcelain specimens is successfully demonstrated. Stress-intensity factors were evaluated from experimental data and also using a three-dimensional finite element analysis. For the unglazed specimen, both experimental and numerical stress-intensity factors are in good agreement with an analytical solution published in the literature. A finite element model is introduced to simulate the thermal stress field created by the glaze. The effective stress-intensity factor obtained from the experiments performed on the glazed specimen agrees reasonably well with that one obtained from the numerical results. For both specimens, the variation of the stress-intensity factor along the crack front was calculated from the finite element analysis.

Concluding, this work illustrates clearly that it is possible in certain technological fracture mechanics problems to achieve quantitative results by means of the speckle photography technique. It also demonstrates the capability of the finite element method to analyse the fracture behaviour of multiphase materials, such as glazed ceramics. Both methods can easily be applied to more complex situations of technological interest.

Acknowledgements

We wish to thank R. Topolevsky for supplying the samples, and M.J. López for data collection and technical assistance.

References

1 **Davidge, R.W.** Mechanical Behaviour of Ceramics, Cambridge University Press, Cambridge, (1979)

2 **Kobayashi, A.S.** (ed.) Experimental Techniques in Fracture Mechanics, Society for Experimental Stress Analysis Monograph No. 2, Westport, Conn. (1975)

3 **Kingery, W.D., Bowen, H.K., Ulhman, D.R.** Introduction to Ceramics, John Wiley, New York, (1976)

4 **Erf, R.K.** (ed.) Speckle Metrology, Academic Press, New York, (1978)

5 **Evans, W.T., Luxmoore, A.** 'Measurements of in-plane displacements around crack tips by a laser speckle method', *Eng Fract Mech* 6, (1974) 735

6 **Chaing, F.P., Asundi, A.** 'White-light speckle method applied to the determination of stress-intensity factor and displacement field around a crack tip', *Eng Fract Mech*, 15 (1981) 115

7 **Kaufmann, G.H., Lopérgolo, A.M., Idelsohn, S.** 'Evaluation of finite element calculations in a cracked cylinder under internal pressure by speckle photography', *ASME Journal of Applied Mechanics*, 50, (1983) 896

8 **Kaufmann, G.H., Idelsohn, S., López, M.J.** 'Measurements of magnification factors for interacting surface flaws by speckle photography', *Proc VII Int Conf Exp Stress Anal* Haifa, Israel, (1982) 580–590

9 **Kaufmann, G.H., Lopergolo, A.M., Idelsohn, S., Barbero, E.** 'Evaluation of finite element calculations in a part circular crack by coherent optics techniques', *Exp Mech*, 27, (1987) 154

10 American Society for Testing Materials, **ASTM Standard E 399-74**, Philadelphia, Penn. (1974)

11 **Barsoum, R.S.** 'Triangular-quarter point elements as elastic and perfectly-plastic crack tip elements', *Int J Num Meth Eng*, 11, (1977) 85

12 **Bueckner, H.F.** 'Weight functions for the notched bar', General Electric Co., Rept. 69-LS-45, (1969)

13 **Kobayashi, A.S.** 'Experimental Techniques in Fracture Mechanics', Society for Experimental Stress Analysis Monograph No. 1, Westport, Conn. (1973)

14 **Raju, I.S., Newman, J.C.** 'Three-dimensional finite element analysis of finite-thickness fracture specimens', National Aeronautics and Space Administration, NASA TN D-8414, (1977)

15 **SAMCEF**, Sisteme d'analyse des milleux continus par elements finis. Manuel d'utilization, Université de Liège

16 **Paris, P.C., Sih, G.C.** 'Stress analysis of cracks', American Society of Testing Materials, ASTM STP 381, (1965)

17 **Dally, J.W., Sciammarella, C.A., Shareef, I.** 'Determination of stress-intensity factor K_I from in-plane displacement measurements', *Proc V Int Cong Exp Mech* Montreal, Canada, (1984) 112–126

18 **Barker, D.B., Sanford, R.J., Chona, R.** 'Determining K and related stress-field parameters from displacement fields', *Exp Mech*, 25, (1985) 399